Improved version of the α-nucleus optical model potential for reactions relevant to the γ process

N. Nhu Le [1,*] and N. Quang Hung [2,3,†]

[1]*Faculty of Physics, University of Education, Hue University, 34 Le Loi Street, Hue City 530000, Vietnam*
[2]*Institute of Fundamental and Applied Sciences, Duy Tan University, Ho Chi Minh City 700000, Vietnam*
[3]*Faculty of Natural Sciences, Duy Tan University, Da Nang City 550000, Vietnam*

The present paper proposes an improved version of the α-nucleus optical model potential (α-OMP), in which the real part of the potential is determined by the double-folding calculation using the density-dependent CDM3Y1 interaction plus a repulsive potential. The imaginary part of the α-OMP is treated by a Woods-Saxon form with energy-dependent depth, while its real part is corrected by including the contribution of the dispersion relation derived from the strong variation of the potential at energies in the vicinity of the Coulomb barrier. The proposed potential is validated by calculating the (α, n) and (α, γ) cross sections on different target nuclei and the obtained results are compared with those predicted by the recent α-OMP suggested by Avrigeanu, as well as the available experimental data. The impacts of the energy-dependent imaginary part and the real dispersive term on the α-induced cross sections are also investigated. The results obtained show that the proposed α-OMP together with that of Avrigeanu describe reasonably well the experimental cross sections of all (α, n) reactions being considered. In addition, the imaginary part of the proposed potential has a strong energy-dependent effect on the α-induced cross section in the energy region below the Coulomb barrier, in particular for radiative α-capture reactions. Two potentials also describe well the cross sections of (α, γ) reactions after rescaling the radiative γ width. This leads to our conclusion that the present α-OMP can provide precise α widths for the study of reactions relevant to the production of p nuclei, and therefore more intensive theoretical research on the radiative strength functions is required.

I. INTRODUCTION

The origin of nuclei in the solar system has been extensively discussed over several decades since the foundations of "Synthesis of the Elements in Stars" were first presented in Ref. [1]. Isotopes located beyond the iron peak can be produced, in principle, by the slow (s) and rapid (r) neutron-capture processes [2]. The s process was found to take place in asymptotic giant branch (AGB) stars [3], whereas binary neutron star mergers [4] and magnetorotationally driven supernova would be considered as candidates for the r process [5]. However, a small number of proton-rich nuclei (p nuclei) observed in nature cannot be formed in neutron-capture nucleosynthesis. Their abundances are supposed to be created during core-collapse and thermonuclear supernovae [6] via photodisintegrations in the γ process, i.e., by (γ, n), (γ, p), and (γ, α) reactions on existing heavy s and r seeds. Despite the tiny amount of p nuclei, their underproduced scenario has not being fully interpreted [7–9].

In fact, explicit explanations of the observed underproductions have yet to be suggested due to the underlying supernova dynamics and the nuclear input parameters, i.e., the astrophysical reaction rates. Narrowing uncertainties in nuclear data is thereby particularly important for a better understanding of the origin of p-nuclei nucleosynthesis. In addition, the experimental measurements of nuclear reaction rates, which are important inputs in modeling thermonuclear burning, have been extensively performed using inverse kinematics [10,11]. In the case of α-induced reactions, the results obtained using different evaluated nuclear libraries such as TALYS [12], NON-SMOKER [13], and SMARAGD [14] have generally exhibited large deviations [15–31]. In particular, the experimental cross sections of (α, γ) reactions were found to be significantly lower than the theoretical predictions [17,19,21,24,29–31]. This disagreement appears more drastically at energies below the Coulomb barrier, where the strong energy dependence of the cross sections is poorly described by the theoretical models. Obviously, the model calculations need to be intensively investigated and their predictive power must be tested using all the available measured data in the relevant mass and energy ranges. Moreover, it is worth noting that one of the key ingredients of the Hauser-Feshbach (HF) statistical model employed in the nuclear libraries is the averaged transmission factors for a light particle to be absorbed or emitted by a compound nucleus (CN). These coefficients are often obtained by solving the Schrödinger equation based on the corresponding particle-nucleus optical potential using the R-matrix [32] or Numerov method [33]. Therefore, both theoretical and experimental studies of the α-nucleus optical model potential (α-OMP) have be-

_____

*nguyennhule@hueuni.edu.vn
†nguyenquanghung5@duytan.edu.vn

come some of the topical issues in nuclear astrophysics [13,24,25,34–40].

Several global and regional α-OMPs have been proposed so far. In the pioneering work by McFadden and Satchler [36], the α-OMP was constructed by using a four-parameter Woods-Saxon (WS) potential, whose parameters were obtained by fitting to the elastic scattering data from a large number of target nuclei at the bombarding energy of 24.7 MeV. This WS type potential with mass- and energy-independent parameters was later used as the default potential in the NON-SMOKER code [13]. Likewise, Demetriou *et al.* [37] introduced a semimicroscopic α-OMP, which consisted of a real part generated from a double-folding model (DFM) [41] together with an imaginary part represented by the WS form [42]. In a later work, Kumar *et al.* [43] proposed a so-called global α-OMP, which was derived from a combination of spherical proton and neutron OMPs in Ref. [44]. Recently, the α-OMP has been significantly improved based on an intensive analysis of high-precision α-particle-induced-reaction data for a large number of target nuclei $45 \leqslant A \leqslant 209$ below the Coulomb barrier [38,39]. This α-OMP, which consists of nine energy-dependent parameters for both real and imaginary parts, has been implemented in the TALYS-1.9 reaction code as one of the default inputs [12]. Although both the aforementioned α-OMPs have described rather well the data in a certain region of target masses and incident energies, many extrapolated parameters have been used, which may lead to some inappropriate descriptions of astrophysical reaction rates, in particular for those in the experimentally inaccessible region. For instance, it has been reported in the recent evaluation of the aforementioned α-OMPs, through reactions involving the α particle on the ^{115}In nucleus at low energies, that further studies of α-OMPs are required to provide a better description for both the elastic scattering and reaction data [16].

The goal of the present work is to develop an α-OMP similar to that proposed in Ref. [37], namely using a real part derived from by the DFM and an imaginary part given in the form of a phenomenological WS potential, but with some additional improvements. First, the real part of the potential is treated based on the density-dependent CDM3Y1 interaction plus the repulsive potential (CDM3Y1+Repulsion) given in our earlier work [45]. This inclusion of the repulsive part is expected to be important for the interaction between the α particle and the targets at the short distances, i.e., close to the center [46]. Second, the imaginary part contains the energy-dependent depth taken from Ref. [47]. In addition, due to the rapid variations in both real and imaginary parts for energies in the vicinity of the Coulomb barrier reported in Refs. [48,49], an energy-dependent and real dispersive contribution such as that proposed in Refs. [50,51] has been added to the present α-OMP. The numerical tests of our α-OMP are carried out for two (α, γ) and (α, n) reactions on many target nuclei, including ^{74}Ge, ^{90,92}Zr, ^{107}Ag, ^{112}Sn, ^{113,115}In, ^{121,123}Sb, ^{127}I, ^{130,132}Ba, ^{151}Eu, ^{162,166}Er, ^{168}Yb, ^{169}Tm, ^{187}Re, and ^{191,193}Ir. Furthermore, although the (α, n) reactions are not directly relevant to the astrophysical production of p nuclei, they will be discussed in the present work as they may provide supplementary evaluations for the proposed α-OMP.

II. THE α-OMP BASED ON THE DOUBLE-FOLDING CDM3Y1+REPULSION

A local and complex OMP $U(r, E)$ between two colliding nuclei can be written via the Feshbach formalism [52]

$$U(r, E) = V_{\text{DF}}(r, E) + \Delta V(r, E) + iW(r, E), \quad (1)$$

where the real part of $V_{\text{DF}}(r, E)$ is obtained from the double-folding (DF) method. This $V_{\text{DF}}(r, E)$ consists of the attractive nuclear potential $V_{\text{N}}(r)$, the repulsive Coulomb potential $V_{\text{C}}(r)$, and the additional repulsive potential $V_{\text{rep.}}(r)$ [45], namely

$$V_{\text{DF}}(r, E) = V_{\text{N}}(r) + V_{\text{C}}(r) + V_{\text{rep.}}(r, E). \quad (2)$$

The quantity $\Delta V(r, E)$ in Eq. (1) denotes the dispersive contribution to the α-OMP, which can be calculated via the following dispersive integral using the imaginary term $W(r, E)$ [50]:

$$\Delta V(r, E) = \frac{\mathcal{P}}{\pi} \int_0^\infty \frac{W(r, E')}{E' - E} dE', \quad (3)$$

where $\mathcal{P}$ stands for the principle value. The imaginary term $W(r, E)$ is written, as usual, in terms of the phenomenological WS form,

$$W(r, E) = -\frac{W(E)}{1 + \exp\left(\frac{r - R_W}{a_W}\right)}, \quad (4)$$

where $R_W = r_W(A_p^{1/3} + A_t^{1/3})$ with $r_W = 1$ and A_p and A_t being the mass numbers of the projectile (p) and target (t) nuclei, respectively. As reported by the measured elastic α-scattering data [24,53], the energy-dependent depth $W(E)$ was found to decrease with increasing energy and it can be approximated by the empirical Fermi-type formula, similar to that presented in Ref. [47]:

$$W(E) = \frac{17 \text{ MeV}}{1 + \exp\left(\frac{0.9E_B - E}{a_E}\right)}, \quad (5)$$

where the relevance of $0.9E_B$ at energies below which the potential parameters must be significantly modified was discussed in Ref. [39]. Moreover, a smaller depth of 17 MeV is employed in the present work instead of 25 MeV as in Eq. (9) of Ref. [47]. The use of this smaller depth is understandable since the real part of the present α-OMP, which is no longer a WS-type function, is modified by using the double-folding CDM3Y1 plus repulsive interaction. In Eq. (5), E and E_B stand for the center-of-mass energy of the projectile and the Coulomb barrier height taken from the shape of the DF potential, respectively, whereas the value of parameter a_E is chosen to be 3 for the α-induced reactions within the mass range considered in the present paper. The diffuseness parameter a_W in Eq. (4) is estimated based on the following relation [54]:

$$E_B \approx \frac{Z_p Z_t e^2}{r_B}\left(1 - \frac{a_W}{r_B}\right), \quad (6)$$

where

$$a_W = r_B - \frac{r_B^2 E_B}{Z_p Z_t e^2}. \quad (7)$$

Here, Z_p and Z_t denote, respectively, the charge numbers of the projectile and target, whereas r_B stands for the barrier position. Since r_B and E_B are determined through the real part of the α-OMP, the diffuseness parameter a_W is also calculated from the DF calculation instead of being a fitting parameter as in Ref. [38].

The attractive nuclear (repulsive Coulomb) potential, $V_{N(C)}(r)$ can be calculated using its general form as [45,55]

$$V_N(r) = \int d\vec{r}_1 d\vec{r}_2 \rho_A^p(\vec{r}_1) F(\rho_A) v_n(s) \rho_A^t(\vec{r}_2), \quad (8)$$

$$V_C(r) = \int d\vec{r}_1 d\vec{r}_2 \rho_{ch.}^p(\vec{r}_1) v_c(s) \rho_{ch.}^t(\vec{r}_2), \quad (9)$$

where $s = |\vec{r}_1 - \vec{r}_2 + \vec{r}|$ is the relative distance between the interacting nucleon pair, whereas $\rho_A^{p(t)}(\vec{r})$ and $\rho_{ch.}^{p(t)}(\vec{r})$ are the nucleon and charge densities of the projectile (target), respectively. In the present calculation, we adopt the nuclear matter (charge) densities of the target and compound nuclei obtained within the Skyrme Hartree-Fock plus BCS (HFBCS) method [56], while the corresponding densities of α particle is given by [57]

$$\rho_A^p = 0.4229 \times \exp(-0.7024r^2), \quad \rho_{ch.}^p = \frac{\rho_A^p}{2}. \quad (10)$$

The effective nucleon-nucleon potential $v_n(s)$ in Eq. (8) is calculated using the Reid parametrization of the Yukawa interaction (M3Y) [55], while the Coulomb term $v_c(s)$ in Eq. (9) is given by a pointlike proton-proton potential [57], namely

$$v_n(s) = 7999 \frac{e^{-4s}}{4s} - 2134 \frac{e^{-2.5s}}{2.5s} - 276\delta(s), \quad (11)$$

$$v_c(s) = \frac{e^2}{4\pi\epsilon_0 s}, \quad (12)$$

where $\delta(s)$ is the zero-range exchange nuclear interaction. The function $F(\rho_A)$ entering in Eq. (8) is a density-dependent nucleon-nucleon interaction, which has the form [55]

$$F(\rho_A) = C\{1 + \alpha \exp(-\beta\rho_A) - \gamma\rho_A\}, \quad (13)$$

with C, α, β, and γ parameters being taken from Table 2 of Ref. [55].

The repulsive potential $V_{rep.}(r, E)$ in Eq. (2) is computed based on the zero-range repulsive nucleon-nucleon potential [45,58],

$$V_{rep.}(r, E) = v_{rep.}(E) \int d\vec{r}_1 d\vec{r}_2 \rho_{rep.}^p(\vec{r}_1) \delta(s) \rho_{rep.}^t(\vec{r}_2), \quad (14)$$

where $\rho_{rep.}^p(\vec{r}_1)$ and $\rho_{rep.}^t(\vec{r}_2)$ are, respectively, the densities of the projectile and target nuclei written in the Fermi-Dirac distribution form with the corresponding repulsive diffuseness parameter $a_{rep.}$, namely

$$\rho_{rep.}^{p(t)}(r) = \frac{\rho_0^{p(t)}}{1 + \exp\left[\frac{r - R_0^{p(t)}}{a_{rep.}}\right]}, \quad (15)$$

with $R_0^{p(t)} = 1.07 A_{p(t)}^{1/3}$ (fm) and $\rho_0^{p(t)}$ being obtained from the normalization condition for the nuclear matter distributions. The repulsive strength $v_{rep.}(E)$ in Eq. (14) is the energy-dependent coefficient, which explicitly depends on the

excitation energy of a compound nucleus determined from the nuclear temperature or the center-of-mass energy of the interacting system. This strength is often determined from the equation of state (EOS) method by assuming that when two nuclei are completely overlapped, the energy of the system will gain an amount of ΔV equal to the total nuclear potential at the origin ($r = 0$) [46,58,59], namely

$$\Delta V = V_N(0) + V_{rep.}(0), \quad (16)$$

$$\Delta V \approx 2A_p[\varepsilon_H(2\rho_0, \delta) - \varepsilon_C(\rho_0, \delta)], \quad (17)$$

where $\varepsilon_{H(C)}$ denotes the hot (cold) nuclear matter EOS given by the Thomas-Fermi formula [60], whereas $\rho_0 = 0.161$ fm^{-3} and $\delta = (\rho_n - \rho_p)/\rho$ [$\rho_{n(p)}$ is the neutron (proton) density and $\rho = \rho_n + \rho_p$] stand for the saturation density and relative neutron excess, respectively. Numerically, ΔV can be obtained by solving a set of two equations $\varepsilon_H = \varepsilon_C + E^*$ (E^* is the excitation energy per nucleon of the compound nucleus) [61] and $K = 18[\varepsilon_C(2\rho_0) - \varepsilon_C(\rho_0)]$ (K is the incompressibility of nuclear matter) [58]. Its final form reads

$$\Delta V = \frac{A_p}{9} K + 2A_p E^*. \quad (18)$$

By using Eqs. (17) and (18) and the relation $E^* = E + Q$ (Q is the reaction Q value), the energy-dependent repulsive strength $v_{rep.}(E)$ is given as

$$v_{rep.}(E) = \frac{2A_p(K/18 + E + Q) - V_N(0)}{V_{rep.}(0)}. \quad (19)$$

III. NUMERICAL RESULTS

The numerical tests of the proposed α-OMP are carried out for the (α, n) and (α, γ) reactions on several target nuclei, ^{74}Ge, ^{90,92}Zr, ^{107}Ag, ^{112}Sn, ^{113,115}In, ^{121,123}Sb, ^{127}I, ^{130,132}Ba, ^{151}Eu, ^{162,166}Er, ^{168}Yb, ^{169}Tm, ^{187}Re, and ^{191,193}Ir. The parameters of the α-OMPs used in the present work for all studied reactions are listed in Table I. As for the diffuseness parameter of the repulsive potential $a_{rep.}$ in Eq. (15), based on our earlier investigation in Ref. [45], a fixed value of $a_{rep.} = 0.35$ fm is chosen for all reactions. The α-OMP in this case consists of six parameters, namely four parameters of the CDM3Y1 interaction, $a_{rep} = 0.35$ fm, and the 17 MeV depth of the imaginary potential. These parameters are fixed for all investigated reactions, which ensures the predictive power of the present α-OMP. The obtained α-OMPs are then used to calculate the transmission coefficients based on the R-matrix method [32]. The (α, n) and (α, γ) cross sections on the aforementioned targets are calculated by implementing the KEWPIE2 code [62]. In the numerical calculations, we adopt the nuclear level density (NLD) model proposed by Reisdorf [63] and the γ-ray strength function (γ-SF) calculated using a simplified version of the modified Lorentzian model (SMLO) [64]. In addition, the global neutron OMPs proposed by Varner et al. [65] are used to calculate the neutron widths.

To test the effect of the dispersive term on the proposed α-OMP, we drop this term, and the potential, in this case, is denoted by α-OMP-NoDis. Similarly, to test the energy dependence of the depth of the imaginary part in Eq. (5),

TABLE I. The parameters of α-OMPs used in the present work for all studied reactions. r_B^0, E_B, and K are the Coulomb barrier radius, barrier height, and nuclear matter incompressibility, respectively.

Reaction	r_B^0 (fm)	E_B (MeV)	K (MeV)
$\alpha + {}^{74}$Ge	8.85	9.70	234.09
$\alpha + {}^{90}$Zr	9.05	11.91	232.42
$\alpha + {}^{92}$Zr	9.12	11.80	232.42
$\alpha + {}^{107}$Ag	8.21	15.10	231.35
$\alpha + {}^{112}$Sn	9.37	14.35	231.86
$\alpha + {}^{113}$In	9.35	14.06	203.12
$\alpha + {}^{115}$In	9.52	13.87	202.55
$\alpha + {}^{121}$Sb	9.60	14.28	205.42
$\alpha + {}^{123}$Sb	9.67	14.18	203.14
$\alpha + {}^{127}$I	9.62	14.80	202.79
$\alpha + {}^{130}$Ba	9.75	15.49	205.29
$\alpha + {}^{132}$Ba	9.77	15.45	203.12
$\alpha + {}^{151}$Eu	10.02	16.96	207.01
$\alpha + {}^{162}$Er	10.17	18.06	214.60
$\alpha + {}^{166}$Er	10.26	17.93	210.04
$\alpha + {}^{168}$Yb	10.26	18.48	213.22
$\alpha + {}^{169}$Tm	10.26	18.17	208.10
$\alpha + {}^{187}$Re	10.41	19.54	196.45
$\alpha + {}^{191}$Ir	10.44	20.03	216.41
$\alpha + {}^{192}$Ir	10.47	19.94	220.12

we set $W(E) = W = 17$ MeV and denote the corresponding potential by α-OMP-Wconst. The validity of the proposed α-OMP is also tested by making a systematic comparison with the results obtained within the recent α-OMP proposed by Avrigeanu (denoted by α-OMP-Avrigeanu) [38] as well as the experimental data.

Figures 1–4 show the (α, n) cross sections as functions of either center-of-mass energy E_{cm} or energy in the laboratory frame E_{lab} calculated within the α-OMP (solid lines) versus those obtained within the α-OMP-NoDis (dotted lines), α-OMP-Wconst (dash-dotted lines), α-OMP-Avrigeanu (dashed lines), and experimental data (filled squares with error bars) for different target nuclei ^{107}Ag, ^{113,115}In, ^{121,123}Sb, ^{127}I, ^{130,132}Ba, ^{151}Eu, ^{162,166}Er, ^{168}Yb, ^{169}Tm, ^{187}Re, and ^{191,193}Ir. Overall, the α-OMP describes rather well all the considered cross-section data. Meanwhile, the cross sections obtained using the α-OMP-NoDis in the energy region below (above) the Coulomb barrier E_B are slightly higher (lower) than those obtained using the α-OMP, except for the ^{113}In$(\alpha, n)^{116}$Sb reaction. For the α-OMP-Wconst, its cross sections at $E_{cm}(E_{lab}) < E_B$ strongly deviate from the α-OMP predictions, while they are close to the α-OMP results at $E_{cm}(E_{lab}) > E_B$. These results indicate that the imaginary part of the α-OMP strongly influences the (α, n) cross sections only in the low-energy region below the Coulomb barrier where the surface absorption has a significant effect, whereas the dispersive factor of the potential has a little contribution to the cross sections at high energies.

To have more intuitive understanding on the influence of the dispersive correction, we plot in Fig. 5 the real parts of the α-OMP at several energies below and above the Coulomb
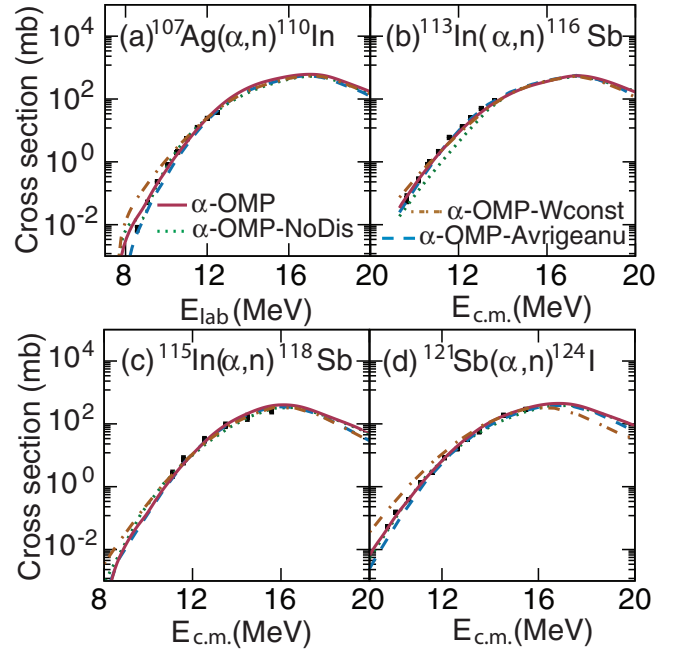

FIG. 1. The (α, n) cross sections obtained using the α-OMP (solid lines), α-OMP-NoDis (dotted lines), α-OMP-Wconst (dash-dotted lines), and α-OMP-Avrigeanu (dashed lines) versus the experimental data taken from Refs. [16,19,29,66] for ^{107}Ag (a), ^{113}In (b), ^{115}In (c), and ^{121}Sb (d) target nuclei.

barrier for the $\alpha + {}^{74}$Ge, $\alpha + {}^{121}$Sb, $\alpha + {}^{151}$Eu, and $\alpha + {}^{187}$Re reactions. It is clear to see in this Fig. 5 that the potential depth is increased with decreasing $E_{cm}(E_{lab})$. At $E_{cm}(E_{lab}) <$

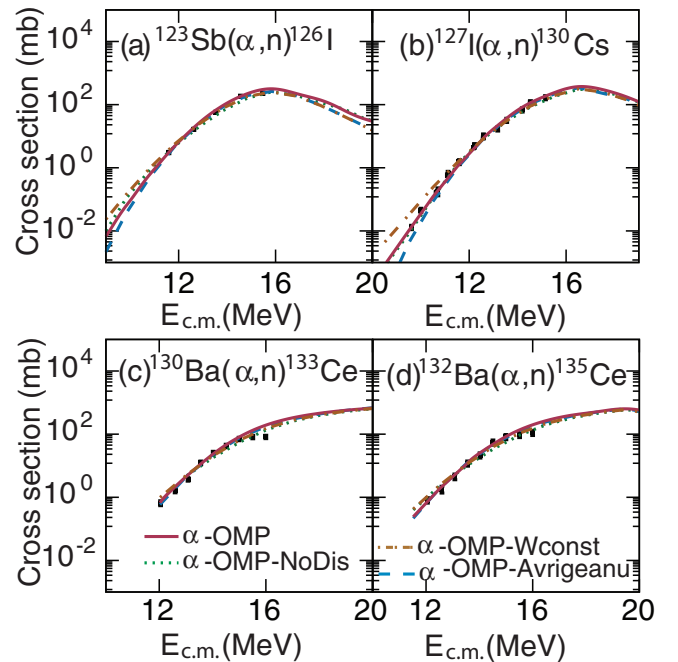FIG. 2. Same as Fig. 1 but for ^{123}Sb (a), ^{127}I (b), ^{130}Ba (c), and ^{132}Ba (d) targets. Experimental data are taken from Refs. [26,66,67].
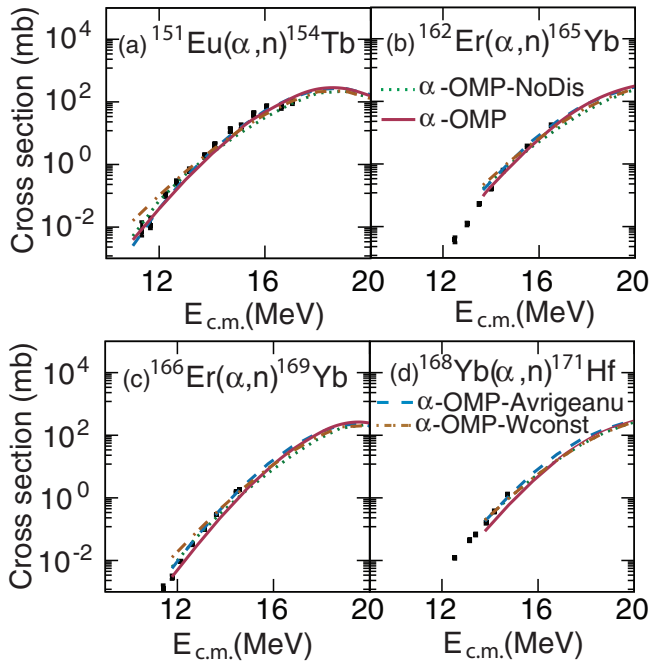
FIG. 3. As Fig. 1 but for ^{151}Eu (a), ^{162}Er (b), ^{166}Er (c), and ^{168}Yb (d) targets. Experimental data are taken from Refs. [21,22,68,69].

FIG. 5. The real parts of the α-OMPs obtained with (broken lines) and without (solid lines) dispersive corrections for $\alpha + {}^{74}$Ge (a), $\alpha + {}^{121}$Sb (b), $\alpha + {}^{151}$Eu (c), and $\alpha + {}^{187}$Re (d) reactions at several energies (E_{1-4}) below and above the Coulomb barrier (E_B).

E_B, the potential depth significantly differs from that obtained without dispersion, while two potentials become closer at $E_{\text{cm}}(E_{\text{lab}}) > E_B$. This behavior explains why the cross sections obtained using the α-OMP-NoDis at $E_{\text{cm}}(E_{\text{lab}})$ in the
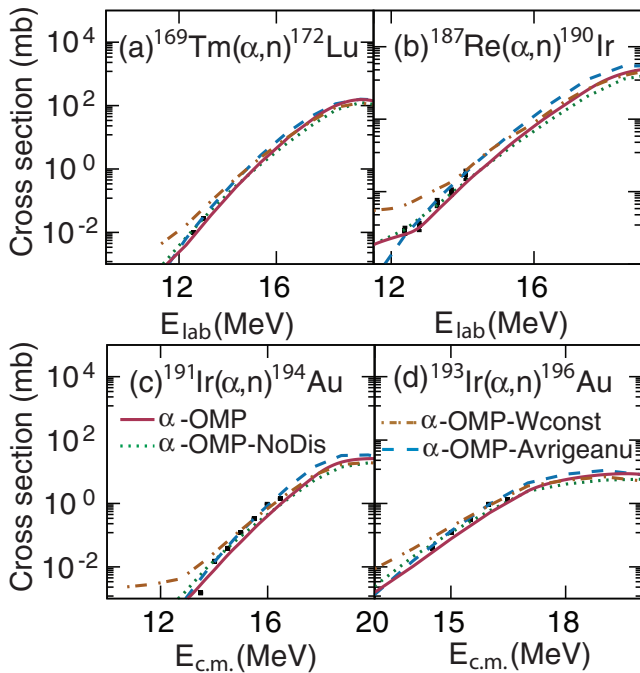

FIG. 4. Same as Fig. 1 but for ^{169}Tm (a), ^{187}Re (b), ^{191}Ir (c), and ^{193}Ir (d) targets. Experimental data are taken from Refs. [17,23,27].
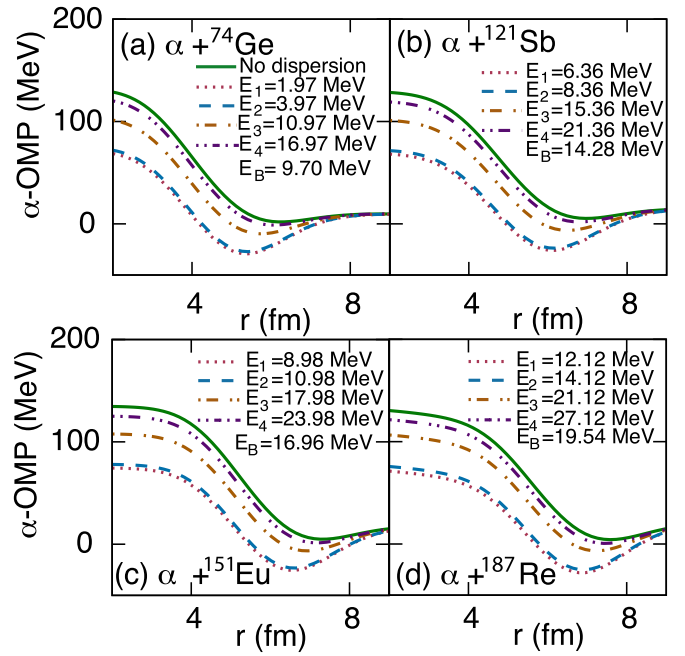
vicinity of the Coulomb barrier are slightly lower than those obtained using the α-OMP, and two potentials predict almost similar cross sections at energies far above the E_B as discussed above. In addition, although the difference between α-OMP and α-OMP-NoDis is significant at low energies (Fig. 5), their predictions on the cross sections only slightly differ in this energy region (Figs. 1–4). This is because the imaginary term has a strong influence on the absorption properties at low energies, so the depth of the shallow pockets has weak accesses to the (α, n) cross sections. As compared to the predictions of the α-OMP-Avrigeanu, the α-OMP provides a slight improvement on the cross-section data. The best results obtained using the present α-OMP are seen for the (α, n) reactions on ^{107}Ag, ^{113,115}In, ^{121,123}Sb, ^{127}I, ^{151}Eu, ^{162}Er, ^{169}Tm, and ^{187}Re targets. This validates the accuracy of the presently proposed α-OMP for the relevant (α, n) reactions.

Figures 6–9 depict the (α, γ) cross sections obtained within the α-OMP, α-OMP-NoDis, α-OMP-Wconst, and α-OMP-Avrigeanu for several reactions. The best-fitted cross sections obtained within some previous analyses [20,66,70] using the TALYS code as well the results obtained using the NON-SMOKER code with default parameters [66] are also displayed in Figs. 6 and 7. The results presented in these figures indicate that although different α-OMPs can describe rather well the cross sections of considered (α, n) reactions, their predictions on the corresponding radiative α-capture reactions reveal some deviations from the measured data. For instance, one can see in Fig. 7(d) that the cross sections of the ^{121}Sb$(\alpha, \gamma)^{124}$I reaction obtained using the NON-SMOKER code with default parameters are about 2–4 times higher than the experimental data [66]. Even the best fitted TALYS calcula-
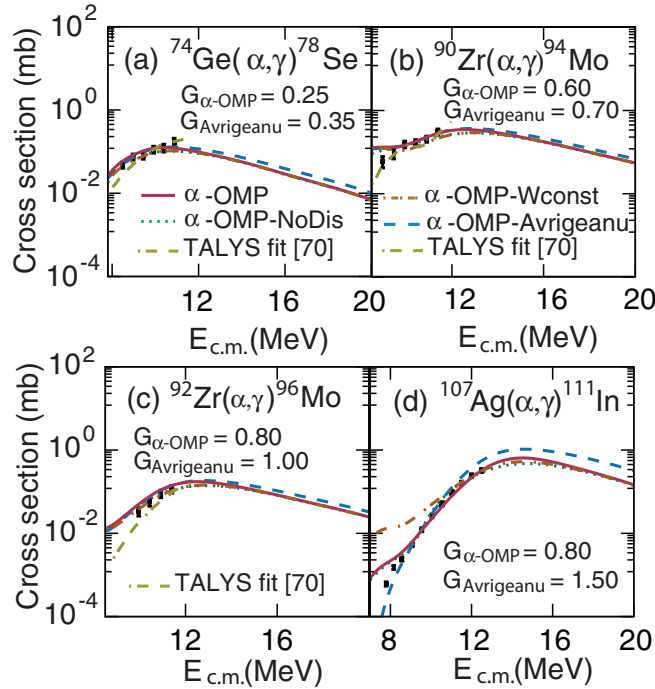
FIG. 6. The (α, γ) cross sections obtained using the α-OMP (solid lines), α-OMP-NoDis (dotted lines), α-OMP-Wconst (dash-dotted lines), and α-OMP-Avrigeanu (dashed lines) versus the experimental data taken from Refs. [19,70] for ^{74}Ge (a), ^{90}Zr (b), ^{92}Zr (c), and ^{107}Ag (d) targets. Some available best fitted cross sections using the TALYS library are also given for reference. The scaling factors for the γ widths used in the calculations with the α-OMP ($G_{\alpha\text{-OPM}}$) and α-OMP-Avrigeanu ($G_{\text{Avrigeanu}}$) are provided in each figure.
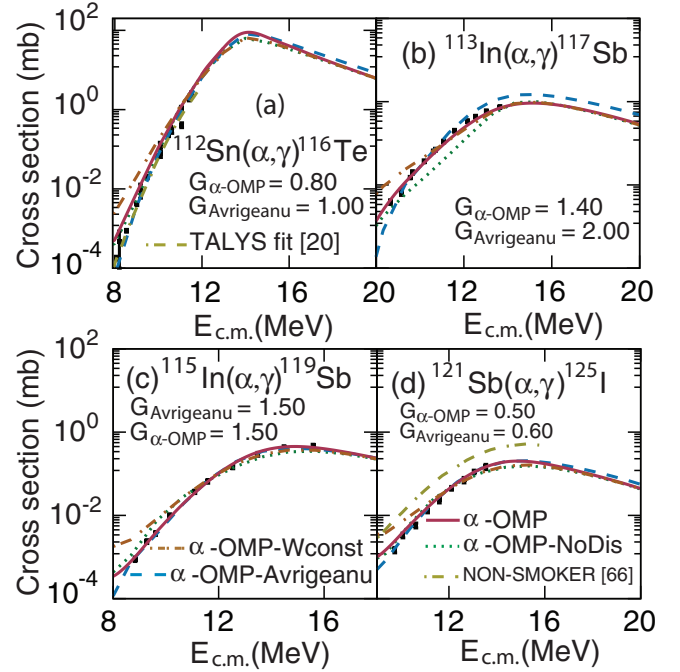

FIG. 7. Same as Fig. 6 but for ^{112}Sn (a), ^{113}In (b), ^{115}In (c), and ^{121}Sb (d) targets. Experimental cross sections are extracted from Refs. [16,20,29,30,66,71]. The best fitted cross sections using the TALYS library and the results obtained using the NON-SMOKER code with default parameters are respectively given in (a) and (d) for reference.
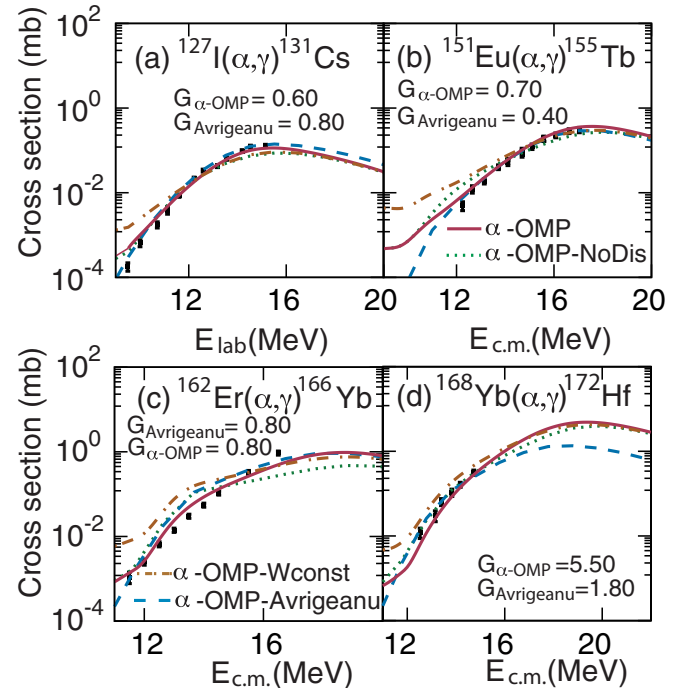
tions still exhibit some deviations from the measured data at low energies [see, e.g., Figs. 6(a) and 6(c)]. This observation implies that while the α width can be described rather well by different OMPs, the discrepancies between the calculated and measured cross sections for the (α, γ) reactions should be due to the neutron and γ widths. Therefore, in the present work, the rescaling factors of the γ width, which are, respectively, denoted by $G_{\alpha\text{-OPM}}$ and $G_{\text{Avrigeanu}}$ for the α-OMP and α-OMP-Avrigeanu potentials, are used to describe the (α, γ) cross sections. The best fitted values of $G_{\alpha\text{-OPM}}$ and $G_{\text{Avrigeanu}}$ for all studied reactions are shown in Figs. 6–9.

It is also seen in Figs. 6–9 that, similarly to the (α, n) reactions, the dispersive factors of the α-OMP have only a minor effect on the (α, γ) cross section. However, the effect of energy-independent depth of the imaginary part at low energies is stronger for the (α, γ) reactions than for the (α, n) ones, namely the (α, γ) cross sections calculated using the energy-independent depth overestimate those obtained using the energy-dependent one as well as the experimental data. This finding is important as it confirms that the depth of the imaginary part of α-OMP should be energy dependent.

The preceding analyses have demonstrated that the proposed α-OPM can provide a good description of the experimental cross sections of (α, n) and (α, γ) reactions (with rescaling factors for the γ width). Furthermore, this α-OMP is

FIG. 8. As in Fig. 6 but for ^{127}I (a), ^{151}Eu (b), ^{162}Er (c), and ^{168}Yb (d) targets. Experimental cross sections are extracted from Refs. [21,22,26,68].
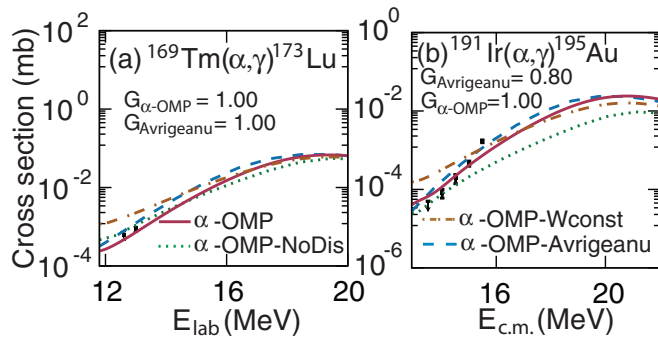
FIG. 9. Same as Fig. 6 but for ^{169}Tm (a) and ^{191}Ir (b) targets. Experimental cross sections are extracted from Refs. [17,27].

more appropriate for studying the α-induced reactions in the higher-mass region due to its derivation from the underlying physics and least free parameters as compared to those of the Avrigeanu potential. For instance, the α-decay half-lives $[\log_{10}(T_\alpha^{1/2})]$ calculated using the real part of the present α-OPM (CDM3Y+repulsion) are, respectively, -2.6291 and -4.0112 for two superheavy nuclei, ^{266}Hs and ^{270}Ds, which are very close to their corresponding experimental values of -2.6383 and -4.0000 [72]. Hence, the real part of the present α-OPM can provide a good description of α-decay properties.

IV. CONCLUSIONS

In the present work, an improved version of the α-nucleus optical model potential (α-OMP) has been proposed for the reactions relevant to the γ process. The proposed potential includes an energy-dependent imaginary part expressed in terms of a phenomenological Woods-Saxon form, while its real part is treated based on the double-folding model (DFM) with the standard density-dependent CDM3Y1 interaction plus a repulsive potential (CDM3Y1+Repulsion). In addition, the potential takes into account also the real dispersive term

derived from the drastic changes in the imaginary and real parts of the potential at energies near the Coulomb barrier. The α-OMPs are then applied to describe the (α, γ) and (α, n) cross sections on twenty target nuclei in the intermediate and heavy mass regions. The results obtained are compared with those calculated within the Avrigeanu potential, as well as the available experimental data. The impacts of dispersive correction to the real part and the energy dependence of the imaginary part on the α-induced cross sections have also been investigated.

It has been found that the α-induced cross sections are extremely sensitive to the imaginary part of the potential, particularly in the case of (α, γ) reactions at energies below the Coulomb barrier. Moreover, the (α, γ) cross sections calculated within the α-OMP with the energy-independent imaginary depth significantly overestimate the experimental data. This observation is consistent with previous findings that the imaginary part of the α-OMP should be energy dependent. Overall, the proposed α-OMP together with that of Avrigeanu nicely describe the measured data of all investigated (α, n) reactions. As for the (α, γ) reactions, both theoretically calculated cross sections reproduce reasonably well the experimental data after scaling the radiative γ width. This implies that the present α-OPM can provide accurate α widths for theoretical studies of the production of p nuclei, hence more theoretical research on the radiative strength functions is recommended. Moreover, the proposed α-OPM is more suitable for investigating the α-induced reactions in the higher-mass region as it is derived from the underlying physics and has fewer adjustable parameters than the Avrigeanu potential.

[1] E. M. Burbidge, G. R. Burbidge, W. A. Fowler, and F. Hoyle, Rev. Mod. Phys. **29**, 547 (1957).

[2] B. S. Meyer, Annu. Rev. Astron. Astrophys. **32**, 153 (1994).

[3] O. Straniero, R. Gallino, M. Busso, A. Chiefei, C. M. Raiteri, M. Limongi, and M. Salaris, Astrophys. J. **440**, L85 (1995).

[4] S. Wanajo, Y. Sekiguchi, N. Nishimura, K. Kiuchi, K. Kyutoku, and M. Shibata, Astrophys. J. Lett. **789**, L39 (2014).

[5] N. Nishimura, T. Takiwaki, and F.-K. Thielemann, Astrophys. J. **810**, 109 (2015).

[6] M. Pignatari, K. Göbe, R. Reifarth, and C. Travaglio, Int. J. Mod. Phys. E **25**, 1630003 (2016).

[7] M. Rayet, N. Prantzos, and M. Arnould, Astron. Astrophys. **227**, 271 (1990).

[8] M. Rayet, M. Arnould, M. Hashimoto, N. Prantzos, and K. Nomoto, Astron. Astrophys. **298**, 517 (1995).

[9] T. Rauscher, A. Heger, R. D. Hoffman, and S. E. Woosley, Astrophys. J. **576**, 323 (2002).

[10] J. Fallis *et al.*, Phys. Lett. B **807**, 135575 (2020).

[11] B. Mei, T. Aumann, S. Bishop, K. Blaum, K. Boretzky, F. Bosch, C. Brandau, H. Bräuning, T. Davinson, I. Dillmann, C. Dimopoulou, O. Ershova, Zs. Fülöp, H. Geissel, J. Glorius, G. Gyürky, M. Heil, F. Käppeler, A. Kelic-Heil, C. Kozhuharov *et al.*, Phys. Rev. C **92**, 035803 (2015).

[12] A. J. Koning and D. Rochman, Nucl. Data Sheets. **113**, 2841 (2012).

[13] T. Rauscher and F.-K. Thielemann, At. Data Nucl. Data Tables **79**, 47 (2001).

[14] T. Rauscher, Computer code SMARAGD, Version 0.9.3s, 2015.

[15] T. Szücs, P. Mohr, Gy. Gyürky, Z. Halász, R. Huszánk, G. G. Kiss, T. N. Szegedi, Zs. Török, and Zs. Fülöp, Phys. Rev. C **100**, 065803 (2019).

[16] G. G. Kiss, T. Szücs, P. Mohr, Zs. Török, R. Huszánk, Gy. Gyürky, and Zs. Fülöp, Phys. Rev. C **97**, 055803 (2018).

[17] T. Szücs, G. Kiss, G. Gyürky, Z. Halász, Zs. Fülöp, and T. Rauscher, Phys. Lett. B **776**, 396 (2018).

[18] Z. Halász, E. Somorjai, G. Gyürky, Z. Elekes, Zs. Fülöp, T. Szücs, G. G. Kiss, N.T. Szegedi, T. Rauscher, J. Görres, and M. Wiescher, Phys. Rev. C **94**, 045801 (2016).

[19] C. Yalçin, G. Gyürky, T. Rauscher, G. G. Kiss, N. Özkan, R. T. Güray, Z. Halász, T. Szücs, Zs. Fülöp, J. Farkas, Z. Korkulu, and E. Somorjai, Phys. Rev. C **91**, 034610 (2015).

[20] L. Netterdon, J. Mayer, P. Scholz, and A. Zilges, Phys. Rev. C **91**, 035801 (2015).

[21] G. G. Kiss, T. Szücs, T. Rauscher, Zs. Török, Zs. Fülöp, Gy. Gyürky, Z. Halász, and E. Somorjai, Phys. Lett. B **735**, 40 (2014).

[22] L. Netterdon, P. Demetriou, J. Endres, U. Giesen, G. G. Kiss, A. Sauerwein, T. Szücs, K. O. Zell, and A. Zilges, Nucl. Phys. A **916**, 149 (2013).

[23] P. Scholz, A. Endres, A. Hennig, L. Netterdon, H. W. Becker, J. Endres, J. Mayer, U. Giesen, D. Rogalla, F. Schlüter, S. G. Pickstone, K. O. Zell, and A. Zilges, Phys. Rev. C **90**, 065807 (2014).

[24] A. Palumbo, W. P. Tan, J. Görres, A. Best, M. Couder, R. Crowter, R. J. deBoer, S. Falahat, P. J. LeBlanc, H. Y. Lee, S. O'Brien, E. Strandberg, M. Wiescher, J. P. Greene, Zs. Fülöp, G. G. Kiss, E. Somorjai, N. Özkan, G. Efe, and R. T. Güray, Phys. Rev. C **85**, 035808 (2012).

[25] P. Mohr, G. Kiss, Z. Fülöp, D. Galaviz, G. Gyürky, and E. Somorjai, At. Data Nucl. Data Tables **99**, 651 (2013).

[26] G. G. Kiss, T. Szücs, Zs. Török, Z. Korkulu, Gy. Gyürky, Z. Halász, Zs. Fülöp, E. Somorjai, and T. Rauscher, Phys. Rev. C **86**, 035801 (2012).

[27] T. Rauscher, G. G. Kiss, T. Szücs, Zs. Fülöp, C. Fröhlich, Gy. Gyürky, Z. Halász, Zs. Kertész, and E. Somorjai, Phys. Rev. C **86**, 015804 (2012).

[28] Z. Korkulu, N. Özkan, G. G. Kiss, T. Szücs, Zs. Fülöp, R. T. Güray, Gy. Gyürky, Z. Halász, E. Somorjai, Zs. Török, and C. Yalçin, J. Phys.: Conf. Ser. **665**, 012042 (2016).

[29] C. Yalcin, R. T. Guray, N. Ozkan, S. Kutlu, G. Gyurky, J. Farkas, G. G. Kiss, Z. Fülöp, A. Simon, E. Somorjai, and T. Rauscher, Phys. Rev. C **79**, 065801 (2009).

[30] W. Rapp, I. Dillmann, F. Käppeler, U. Giesen, H. Klein, T. Rauscher, D. Hentschel, and S. Hilpp, Phys. Rev. C **78**, 025804 (2008).

[31] G. Gyurky, G. G. Kiss, Z. Elekes, Zs. Fülöp, E. Somorjai, A. Palumbo, J. Gorres, H. Y. Lee, W. Rapp, M. Wiescher, N. Ozkan, R.T. Guray, G. Efe, and T. Rauscher, Phys. Rev. C **74**, 025805 (2006).

[32] P. Descouvemont, Comput. Phys. Commun. **200**, 199 (2016).

[33] K. Hagino, N. Rowley, and A. Kruppa, Comput. Phys. Commun. **123**, 143 (1999).

[34] A. Ornelas *et al.*, Nucl. Phys. A **940**, 194 (2015).

[35] G. G. Kiss, P. Mohr, Zs. Fülöp, D. Galaviz, G. Gyurky, Z. Elekes, E. Somorjai, A. Kretschmer, K. Sonnabend, A. Zilges, and M. Avrigeanu, Phys. Rev. C **80**, 045807 (2009).

[36] L. McFadden and G. Satchler, Nucl. Phys. **84**, 177 (1966).

[37] P. Demetriou, C. Grama, and S. Goriely, Nucl. Phys. A **707**, 253 (2002).

[38] V. Avrigeanu, M. Avrigeanu, and C. Mǎnǎilescu, Phys. Rev. C **90**, 044612 (2014).

[39] M. Avrigeanu and V. Avrigeanu, Phys. Rev. C **82**, 014606 (2010).

[40] J. Glorius, K. Sonnabend, J. Görres, D. Robertson, M. Knörzer, A. Kontos, T. Rauscher, R. Reifarth, A. Sauerwein, E. Stech, W. Tan, T. Thomas, and M. Wiescher, Phys. Rev. C **89**, 065808 (2014).

[41] A. Kobos, B. Brown, R. Lindsay, and G. Satchler, Nucl. Phys. A **425**, 205 (1984).

[42] T. Mayer-Kuckuk, *Kernphysik* (Vieweg+Teubner Verlag, Wiesbaden, 2002).

[43] A. Kumar, S. Kailas, S. Rathi, and K. Mahata, Nucl. Phys. A **776**, 105 (2006).

[44] S. Watanabe, Nucl. Phys. A **8**, 484 (1958).

[45] N. NhuLe, N. Ngoc Duy, and N. Quang Hung, Eur. Phys. J. A **57**, 187 (2021).

[46] Ş. Mişicu and H. Esbensen, Phys. Rev. Lett. **96**, 112701 (2006).

[47] A. Sauerwein, H. W. Becker, H. Dombrowski, M. Elvers, J. Endres, U. Giesen, J. Hasper, A. Hennig, L. Netterdon, T. Rauscher, D. Rogalla, K. O. Zell, and A. Zilges, Phys. Rev. C **84**, 045808 (2011).

[48] A. Baeza, B. Bilwes, R. Bilwes, J. Díaz, and J. L. Ferrero, Nucl. Phys. A **419**, 412 (1984).

[49] J. S. Lilley, B. R. Fulton, M. A. Nagarajan, I. S. Thompson, and D. W. Banes, Phys. Lett. B **151**, 181 (1985).

[50] C. Mahaux, H. Ngô, and G. R. Satchler, Nucl. Phys. A **449**, 354 (1986).

[51] V. Durant, P. Capel, and A. Schwenk, Phys. Rev. C **102**, 014622 (2020).

[52] H. Feshbach, *Theoretical Nuclear Physics* (Wiley, New York, 1992).

[53] U. Atzrott, P. Mohr, H. Abele, C. Hillenmayer, and G. Staudt, Phys. Rev. C **53**, 1336 (1996).

[54] G. Goldring, M. Samuel, B. Watson, M. Bertin, and S. Tabor, Phys. Lett. B **32**, 465 (1970).

[55] I. I. Gontchar and M. V. Chushnyakova, Comput. Phys. Commun. **181**, 168 (2010).

[56] G. Colò, L. Cao, N. Van Giai, and L. Capelli, Comput. Phys. Commun. **184**, 142 (2013).

[57] G. R. Satchler and W. G. Love, Phys. Rep. **55**, 183 (1979).

[58] F. Ghorbani, S. A. Alavi, V. Dehghani, A. Soylu, and F. Koyuncu, Phys. Rev. C **102**, 014610 (2020).

[59] S. Misicu and H. Esbensen, Phys. Rev. C **75**, 034606 (2007).

[60] W. D. Myers and W. J. Świątecki, Phys. Rev. C **57**, 3020 (1998).

[61] M. Abd-Alla, Acta Phys. Pol. B **23**, 807 (1992).

[62] H. Lü, A. Marchix, Y. Abe, and D. Boilley, Comput. Phys. Commun. **200**, 381 (2016).

[63] W. Reisdorf, Z. Phys. A **300**, 227 (1981).

[64] V. Plujko, R. Capote, and O. Gorbachenko, At. Data Nucl. Data Tables **97**, 567 (2011).

[65] R. Varner, W. Thompson, T. McAbee, E. Ludwig, and T. Clegg, Phys. Rep. **201**, 57 (1991).

[66] Z. Korkulu, N. Ozkan, G.G. Kiss, T. Szucs, G. Gyurky, Zs. Fülöp, R. T. Guray, Z. Halasz, T. Rauscher, E. Somorjai, Z. Torok, and C. Yalcin, Phys. Rev. C **97**, 045803 (2018).

[67] Z. Halász, Gy. Gyürky, J. Farkas, Zs. Fülöp, T. Szücs, E. Somorjai, and T. Rauscher, Phys. Rev. C **85**, 025804 (2012).

[68] Gy. Gyürky, Z. Elekes, J. Farkas, Zs. Fülöp, Z. Halász, G. G. Kiss, E. Somorjai, T. Szücs, R. T. Güray, and N. Özkan, J. Phys. G **37**, 115201 (2010).

[69] G. G. Kiss, T. Szücs, T. Rauscher, Zs. Török, L. Csedreki, Zs. Fülöp, G. Gyürky, and Z. Halász, J. Phys. G **42**, 055103 (2015).

[70] S. J. Quinn, A. Spyrou, A. Simon, A. Battaglia, M. Bowers, B. Bucher, C. Casarella, M. Couder, P. A. DeYoung, A. C. Dombos, J. Gorres, A. Kontos, Q. Li, A. Long, M. Moran, N. Paul, J. Pereira, D. Robertson, K. Smith, M. K. Smith, E. Stech, R. Talwar, W. P. Tan, and M. Wiescher, Phys. Rev. C **92**, 045805 (2015).

[71] N. Ozkan, G. Efe, R. T. Guray, A. Palumbo, J. Gorres, H. Y. Lee, L. O. Lamm, W. Rapp, E. Stech, M. Wiescher, G. Gyurky, Zs. Fülöp, and E. Somorjai, Phys. Rev. C **75**, 025801 (2007).

[72] Nuclear Wallet Cards Search, https://www.nndc.bnl.gov/nudat2/indx_sigma.jsp.